During the structure determination the formula was originally thought to correspond to a tetrahydrate with two general positions occupied by water molecules, but during refinement very high thermal factors were observed for these water molecules and, in addition, an abnormally short distance between them. In fact, as already observed in $Na_2Cd_2P_6O_{18}\cdot 14H_2O$ (Averbuch-Pouchot, 1990), the water molecules are statistically distributed on two general positions denoted here as O(*W*1) and O(*W*2). After refinements of the occupancy rates of these two positions: O(*W*1) 0·783 (4), O(*W*2) 0·236 (4), the title compound appears to be really a dihydrate and the thermal factors decrease to values one can expect for this type of salt.

The main interatomic distances observed in this arrangement and the geometry of the hydrogen-bond scheme are reported in Table 2.

Fig. 1 is a projection along the *c* axis of this atomic arrangement, drawn using the *STRUPLO* program (Fischer, 1985).

References

AVERBUCH-POUCHOT, M. T. (1989). *C. R. Acad. Sci.* **308**(II), 1699–1702.

AVERBUCH-POUCHOT, M. T. (1990). *Acta Cryst.* C**46**, 10–13.

BOUDJADA, N. (1985). Thesis, Univ. of Grenoble, France.

Enraf–Nonius (1977). *Structure Determination Package*, version RSX11M. Enraf–Nonius, Delft, The Netherlands.

FISCHER, R. X. (1985). *J. Appl. Cryst.* **18**, 258–262.

International Tables for X-ray Crystallography (1974). Vol. IV, Table 2.2B. Birmingham: Kynoch Press. (Present distributor Kluwer Academic Publishers, Dordrecht.)

MAIN, P., HULL, S. E., LESSINGER, L., GERMAIN, G., DECLERCQ, J.-P. & WOOLFSON, M. M. (1977). *MULTAN77. A System of Computer Programs for the Automatic Solution of Crystal Structures from X-ray Diffraction Data.* Univs. of York, England, and Louvain, Belgium.

Acta Cryst. (1990). C**46**, 181–186

Structural Phase Transitions in Chevrel Phases Containing Divalent Metal Cations. II. Structure Refinement of Triclinic $EuMo_6S_8$ and $BaMo_6S_8$ at Low Temperature

BY F. KUBEL* AND K. YVON†

Laboratoire de Cristallographie aux Rayons X, Université de Genève, 24 quai Ernest-Ansermet, CH-1211 Genève 4, Switzerland

(*Received* 8 *February* 1989; *accepted* 12 *May* 1989)

Abstract. Single-crystal X-ray ($\lambda = 0{\cdot}71069$ Å) diffraction data above and below the lattice transformation temperature, T_t, are reported for $EuMo_6S_8$ ($T_t = 110$ K) and $BaMo_6S_8$ ($T_t = 175$ K): $EuMo_6S_8$, $M_r = 984{\cdot}1$, $T = 112$ K: rhombohedral, $R\bar{3}$, $a = 6{\cdot}5378$ (5) Å, $\alpha = 88{\cdot}809$ (11)°, $V = 279{\cdot}26$ (7) Å^3, $Z = 1$, $D_x = 5{\cdot}862$ Mg m^{-3}, $\mu = 13{\cdot}33$ mm^{-1}, $F(000) = 443$, $R(wR) = 0{\cdot}038$ (0·075) for 25 variables and 977 independent reflections; $T = 40$ K: triclinic, $P\bar{1}$, $a = 6{\cdot}4692$ (16), $b = 6{\cdot}5651$ (13), $c = 6{\cdot}5986$ (10) Å, $\alpha = 89{\cdot}179$ (15), $\beta = 89{\cdot}184$ (16), $\gamma = 88{\cdot}009$ (20)°, $V = 280{\cdot}02$ (18) Å^3, $Z = 1$, $D_x = 5{\cdot}836$ Mg m^{-3}, $\mu = 13{\cdot}33$ mm^{-1}, $R(wR) = 0{\cdot}058$ (0·061) for 71 variables and 1637 independent reflections. $BaMo_6S_8$, $M_r = 969{\cdot}5$, $T = 177$ K: rhombohedral, $R\bar{3}$, $a = 6{\cdot}6441$ (6) Å, $\alpha = 88{\cdot}562$ (8)°, $V = 293{\cdot}02$ (8) Å^3, $Z = 1$, $D_x = 5{\cdot}494$ Mg m^{-3}, $\mu = 10{\cdot}71$ mm^{-1}, $F(000) = 436$, $R(wR) = 0{\cdot}060$ (0·043) for 25 variables and 858 independent reflections; $T = 173$ K: triclinic, $P\bar{1}$, $a = 6{\cdot}5896$ (4), $b = 6{\cdot}6500$ (5), $c = 6{\cdot}6899$ (5) Å, $\alpha = 88{\cdot}731$ (7), $\beta = 88{\cdot}818$ (7), $\gamma = 88{\cdot}059$ (7)°, $V = 292{\cdot}86$ (7) Å^3, $Z = 1$, $D_x = 5{\cdot}497$ Mg m^{-3}, $\mu = 10{\cdot}71$ mm^{-1}, $R(wR) = 0{\cdot}070$ (0·060) for 30 variables and 1686 independent reflections. For $EuMo_6S_8$ the bond and contact distances of the triclinic modification differ from those of the rhombohedral modification by up to 0·0410 (14) (Mo—Mo), 0·032 (6) (Mo—S), 0·033 (3) (Eu—S) and 0·084 (4) Å (S—S). For $BaMo_6S_8$ they differ by up to 0·33 (2) (Mo—Mo), 0·021 (5) (Mo—S), 0·028 (4) (Ba—S) and 0·066 (6) Å (S—S). The cell volume of $EuMo_6S_8$ at the rhombohedral-to-triclinic phase transition increases by about 0·83 (15) Å^3 whereas that of $BaMo_6S_8$ remains constant within experimental resolution (0·2 Å^3).

Introduction. Chevrel phase sulfides MMo_6S_8 containing divalent metal cations such as M = Eu, Sr, Ba undergo structural phase transitions below room temperature (Baillif, Dunand, Muller & Yvon, 1981; Baillif, Junod, Lachal, Muller & Yvon, 1981; Lachal, Baillif, Junod & Muller, 1983). Structural parameters

* Now at Département de Chimie Minérale, Analytique et Appliquée, Université de Genève.

† Also at Institut für Physikalische und Theoretische Chemie, Technische Universität, Graz, Austria.

0108-2701/90/020181-06$03.00

Table 1. *Experimental conditions and agreement factors for* MMo_6S_8 (M = Eu,Ba) *at various temperatures*

	$EuMo_6S_8$		$BaMo_6S_8$	
Temperature (K)	112	40	177	173
Space group	$R\bar{3}$	$P\bar{1}$	$R\bar{3}$	$P\bar{1}$
Determination of lattice parameters				
Number of reflections	25	25	25	25
θ range (°)	22–28	25–29	30–36	27–29
Crystal radius (mm)	0·17	0·20		
Crystal cube length (mm)			0·18	0·06
$(\sin\theta/\lambda)_{max}$ (Å^{-1})	1·27	0·90	1·06	1·08
Range of hkl				
h	0→11	−11→11	1→10	0→14
k	0→11	−11→11	−9→10	−9→9
l	−11→11	0→11	−9→9	−8→8
Standard reflections	$3\bar{2}7$	$3\bar{6}4$	$\bar{3}0\bar{1}$	221
	$\bar{1}47$	$46\bar{1}$	$\bar{1}\bar{3}0$	$1\bar{1}3$
				$13\bar{2}$
Number of reflections				
measured	2012	3666	3149	2090
Number of unobserved				
$[I < 3\sigma(I)]$ reflections	206	1547	1172	404
Refinement program system	*SDP*	*XRAY*	*XRAY*	*XRAY*
R_{int}	0·019	—	0·048	—
Max. shift/e.s.d.	$< 10^{-2}$	$< 10^{-1}$	$< 10^{-2}$	$< 10^{-2}$
Scan type	ω–2θ	ω–2θ	ω–2θ	ω–2θ
Scan speed (° min^{-1})	3·5–5·5*	3·5–5·5*	3·5–5·5*	3·0
R	0·038	0·058	0·060	0·070
wR	0·075	0·061	0·043	0·060
Number of variables	25	71	25	30
Number of independent reflections	977	1637	858	1686
Goodness-of-fit	2·9	2·70	3·61	2·22
Extinction coefficient (° × 10^{-6})	1·80 (16)	2·3 (5)	2·1 (3)	—

* Depending on prescan intensity.

Table 2. *Atomic coordinates and anisotropic thermal parameters* U_{ij} (Å^2 × 10^2) *of* $EuMo_6S_8$ *and* $BaMo_6S_8$ *at various temperatures*

The expression of the temperature factor is $\exp[-2\pi^2(h^2a^{*2}U_{11} + k^2b^{*2}U_{22} + l^2c^{*2}U_{33} + hka^*b^*2U_{12} + hla^*c^*2U_{13} + klb^*c^*2U_{23})]$, where a^*, b^*, c^* are reciprocal-lattice constants.

	$EuMo_6S_8$		$BaMo_6S_8$	
Temperature (K)	112	40	177	173
Space group	$R\bar{3}$†	$P\bar{1}$	$R\bar{3}$†	$P\bar{1}$
Eu,Ba in	1*a*[0,0,0]	1*a*[0,0,0]	1*a*[0,0,0]	1*a*[0,0,0]
U_{11}	0·45 (1)	0·807 (23)	0·99 (3)	0·649 (17)
U_{22}	0·45	0·57 (5)	0·99	
U_{33}	0·45	0·613 (20)	0·99	
U_{12}	−0·21 (1)	−0·257 (21)	−0·247 (25)	
U_{13}	−0·21	−0·227 (13)	−0·247	
U_{23}	−0·21	−144 (17)	−0·247	
Mo(1) in	6*f*[*x*,*y*,*z*]	2*i*[*x*,*y*,*z*]	6*f*[*x*,*y*,*z*]	2*i*[*x*,*y*,*z*]
x	0·22840 (8)	0·23322 (11)	0·23479 (16)	0·23750 (16)
y	0·56297 (8)	0·56160 (16)	0·56589 (16)	0·56443 (19)
z	0·41866 (8)	0·42152 (9)	0·41741 (16)	0·41916 (14)
U_{11}	0·18 (2)	0·695 (25)	0·76 (5)	0·383 (15)
U_{22}	0·16 (2)	0·40 (6)	0·66 (4)	
U_{33}	0·14 (2)	0·562 (22)	0·64 (4)	
U_{12}	−0·08 (1)	−0·218 (25)	−0·150 (25)	
U_{13}	−0·03 (1)	−0·206 (15)	−0·11 (3)	
U_{23}	−0·06 (1)	−0·076 (19)	−0·10 (3)	
Mo(2) in		2*i*[*x*,*y*,*z*]		2*i*[*x*,*y*,*z*]
x		0·41918 (11)		0·41765 (16)
y		0·22702 (16)		0·23305 (18)
z		0·56285 (9)		0·56528 (14)
U_{11}		0·696 (25)		0·357 (15)
U_{22}		0·47 (6)		
U_{33}		0·550 (22)		
U_{12}		−0·202 (25)		
U_{13}		−0·179 (16)		
U_{23}		−0·074 (20)		

Table 2 (*cont.*)

	$EuMo_6S_8$		$BaMo_6S_8$	
Temperature (K)	112	40	177	173
Space group	$R\bar{3}$†	$P\bar{1}$	$R\bar{3}$†	$P\bar{1}$
Mo(3) in		2*i*[*x*,*y*,*z*]		2*i*[*x*,*y*,*z*]
x		0·56450 (11)		0·56678 (16)
y		0·41778 (16)		0·41669 (18)
z		0·22751 (9)		0·23264 (14)
U_{11}		0·739 (25)		0·371 (15)
U_{22}		0·50 (6)		
U_{33}		0·543 (23)		
U_{12}		−0·220 (24)		
U_{13}		−0·223 (16)		
U_{23}		−0·045 (19)		
S(1) in	6*f*[*x*,*y*,*z*]	2*i*[*x*,*y*,*z*]	6*f*[*x*,*y*,*z*]	2*i*[*x*,*y*,*z*]
x	0·12444 (25)	0·1250 (3)	0·1233 (5)	0·1240 (5)
y	0·38158 (25)	0·3822 (5)	0·3907 (5)	0·3924 (6)
z	0·74434 (25)	0·7460 (3)	0·7365 (5)	0·7369 (4)
U_{11}	0·22 (5)	0·83 (7)	0·75 (12)	0·55 (4)
U_{22}	0·34 (5)	0·57 (18)	1·14 (13)	
U_{33}	0·35 (5)	0·74 (6)	1·11 (13)	
U_{12}	−0·13 (4)	−0·20 (8)	−0·21 (8)	
U_{13}	−0·05 (4)	−0·16 (5)	−0·08 (8)	
U_{23}	−0·05 (4)	−0·03 (6)	−0·07 (9)	
S(2) in	2*c*[*x*,*x*,*x*]	2*i*[*x*,*y*,*z*]	2*c*[*x*,*x*,*x*]	2*i*[*x*,*y*,*z*]
x	0·2449 (7)	0·2511 (3)	0·2512 (3)	0·2556 (5)
y	0·2449	0·2400 (5)	0·2512	0·2469 (6)
z	0·2449	0·2457 (3)	0·2512	0·2524 (4)
U_{11}	0·4 (1)	0·99 (7)	1·06 (9)	0·77 (5)
U_{22}	0·4	0·32 (18)	1·06	
U_{33}	0·4	0·73 (6)	1·06	
U_{12}	−0·01 (1)	−0·37 (8)	−0·24 (7)	
U_{13}	−0·01	−0·28 (5)	−0·24	
U_{23}	−0·01	−0·15 (6)	−0·24	
S(3) in		2*i*[*x*,*y*,*z*]		2*i*[*x*,*y*,*z*]
x		0·3816 (3)]		0·3915 (5)
y		0·7411 (5)		0·7359 (5)
z		0·1261 (3)		0·1247 (4)
U_{11}		0·88 (7)		0·53 (4)
U_{22}		0·33 (18)		
U_{33}		0·73 (6)		
U_{12}		−0·13 (8)		
U_{13}		−0·31 (5)		
U_{23}		−0·09 (6)		
S(4) in		2*i*[*x*,*y*,*z*]		2*i*[*x*,*y*,*z*]
x		0·7458 (3)		0·7376 (5)
y		0·1230 (5)		0·1224 (5)
z		0·3785 (3)		0·3878 (4)
U_{11}		0·88 (7)		0·55 (4)
U_{22}		0·38 (17)		
U_{33}		0·79 (6)		
U_{12}		−0·23 (8)		
U_{13}		−0·23 (5)		
U_{23}		0·01 (6)		

† Rhombohedral setting.

at room temperature for the rhombohedral high-temperature modification of these compounds were reported in part I of this work (Kubel & Yvon, 1987) and elsewhere (Peña, Horyn, Geantet, Gougeon, Padiou & Sergent, 1986; Jorgensen & Hinks, 1986; Kubel & Yvon, 1988). In the second part of this work we report structure parameters at low temperature, for two members of this series, $EuMo_6S_8$ and $BaMo_6S_8$. Structure parameters for their triclinic low-temperature modifications have so far only been reported from powder diffraction experiments (Jorgensen & Hinks, 1986; Kubel, Yvon, Ihringer & Werner, 1988).

Experimental. The samples used were those described in part I. For $EuMo_6S_8$ various spherical single crystals were prepared in a diamond-coated compressed-air mill whereas for $BaMo_6S_8$ cube-shaped crystals were isolated from a crushed sample. The X-ray measurements on $EuMo_6S_8$ were made on a CAD-4 diffractometer equipped with a prototype of an He-flow cryostat and a liquid-nitrogen cooling device (models FR 558-S and FR 537, Enraf–Nonius, Delft) whereas those on $BaMo_6S_8$ were made on a Philips PW1110 diffractometer equipped with a liquid-nitrogen cooling device, model FR 537 (LEYBOLD). Data sets were collected on four different crystals, each at a different temperature which was either above or below the phase transformation temperature, T_t ($EuMo_6S_8$: $T_t = 110$ K; $BaMo_6S_8$: $T_t = 175$ K). The structures were refined with the *XRAY* program system (Stewart, Machin, Dickinson, Ammon, Heck & Flack, 1976) and *SDP* program system (Frenz, 1983) by applying spherical absorption corrections (max. and min. values 3·73 and 1·52 respectively) and by minimizing the function $\sum w_i(|F_r|_i - |F_c|_i/k_i)^2$ with $w_i = 1/\sigma^2(F_r)_i$. The starting parameters for the positional coordinates of the triclinic modifications were those determined on $EuMo_6S_8$ by powder diffraction at 20 K (Kubel *et al.*, 1988). Atomic scattering factors and anomalous-dispersion factors were taken from *International Tables for X-ray Crystallography*. (1974). The experimental conditions, cell parameters and refinement indices are summarized in Table 1, and the standardized atomic parameters given in Table 2.* Note that as a consequence of the standardization (Gelato & Parthé, 1987) the cell parameters b and c are interchanged with respect to those reported in previous publications (Baillif, Junod *et al.*, 1981; Jorgensen & Hinks, 1986). The $EuMo_6S_8$ data at 40 K were collected on a single crystal which had split into two triclinic individuals at the phase transition. Only data of the larger individual were retained. Of these about 10% were rejected because of contamination by reflections of the smaller individual. After these reflections were included in the structure refinement the residual increased from $R = 0{\cdot}058$ to 0·083.

Lattice parameters as a function of the temperature are represented in Fig. 1. For $EuMo_6S_8$ they were measured on a spherical single crystal in the temperature interval between 293 and 100 K by using the liquid-nitrogen cooling device. For $BaMo_6S_8$ they were measured on a powder sample in the temperature interval between 293 and 20 K by using a low-temperature Guinier film camera (Ihringer, 1982). The data on $EuMo_6S_8$ measured at

* Lists of structure factors have been deposited with the British Library Document Supply Centre as Supplementary Publication No. SUP 52233 (48 pp.). Copies may be obtained through The Executive Secretary, International Union of Crystallography, 5 Abbey Square, Chester CH1 2HU, England.

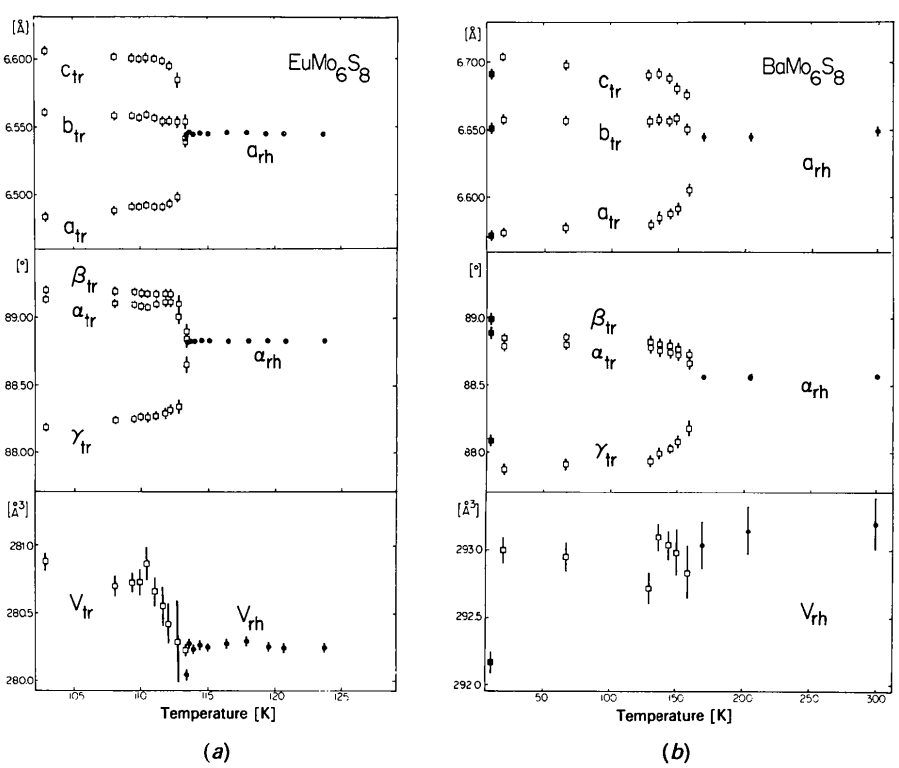

Fig. 1. Rhombohedral and triclinic lattice parameters of (*a*) an $EuMo_6S_8$ single crystal and of (*b*) $BaMo_6S_8$ powder, as a function of temperature. The values for $BaMo_6S_8$ at 10 K (filled squares) are taken from Baillif, Junod *et al.* (1981). Note the different temperature scales in (*a*) and (*b*).

100 K differ by up to 7σ with respect to those reported previously from X-ray powder diffraction work at 14 (Kubel *et al.*, 1988) and 10 K (Baillif, Dunand *et al.*, 1981), and those on $BaMo_6S_8$ at 10 K by up to 13σ with respect to data reported at 10 K from X-ray (Baillif, Dunand *et al.*, 1981) and neutron powder diffraction work (Jorgensen & Hinks, 1986). The reason for these discrepancies are presumably due to differences in stoichiometry. Attempts to refine the triclinic low-temperature structures of the other members of this structural series ($CaMo_6S_8$, $SrMo_6S_8$) failed because the crystals broke up during the structural phase transition. Structural drawings similar to those in part I are represented in Fig. 2, and interatomic distances and angles are listed in Table 3.

Discussion. The structural changes of $EuMo_6S_8$ and $BaMo_6S_8$ during the phase transformation can be summarized as follows. At the transition temperature, T_t, the rhombohedral lattice undergoes a discontinuous triclinic deformation with similar shear directions in both compounds ($a_{tr} < b_{tr} < c_{tr}$, $\gamma_{tr} < \alpha_{tr} < \beta_{tr}$; Fig. 1). Below T_t the deformation of the triclinic lattice continues within a temperature interval, ΔT, that is larger in $BaMo_6S_8$ ($\Delta T \sim 50$ K) than in $EuMo_6S_8$ ($\Delta T \sim 10$ K). However, this difference may not be genuine because the data of the Eu compound refer to a single crystal while those of the Ba compound refer to a powder. At temperatures below 100 K the lattice deformation in $EuMo_6S_8$ is larger than in $BaMo_6S_8$. As expected from the pressure dependence of T_t (Hor, Wu, Lin, Shao, Jin & Chu, 1982) the cell volume, V, increases at T_t upon cooling. For $EuMo_6S_8$ the increase is about $\Delta V \simeq 0{\cdot}83\ (15)$ Å^3, which is slightly larger than predicted ($\Delta V \simeq 0{\cdot}5$ Å^3; Decroux, Torikachvili, Maple, Baillif, Fischer & Muller, 1983) and smaller than measured previously from powder diffraction data ($\Delta V \sim 1$ Å^3; Kubel *et al.*, 1988). For $BaMo_6S_8$ no volume discontinuity at T_t is apparent in Fig. 1. In view of the resolution of the data it is expected to be smaller

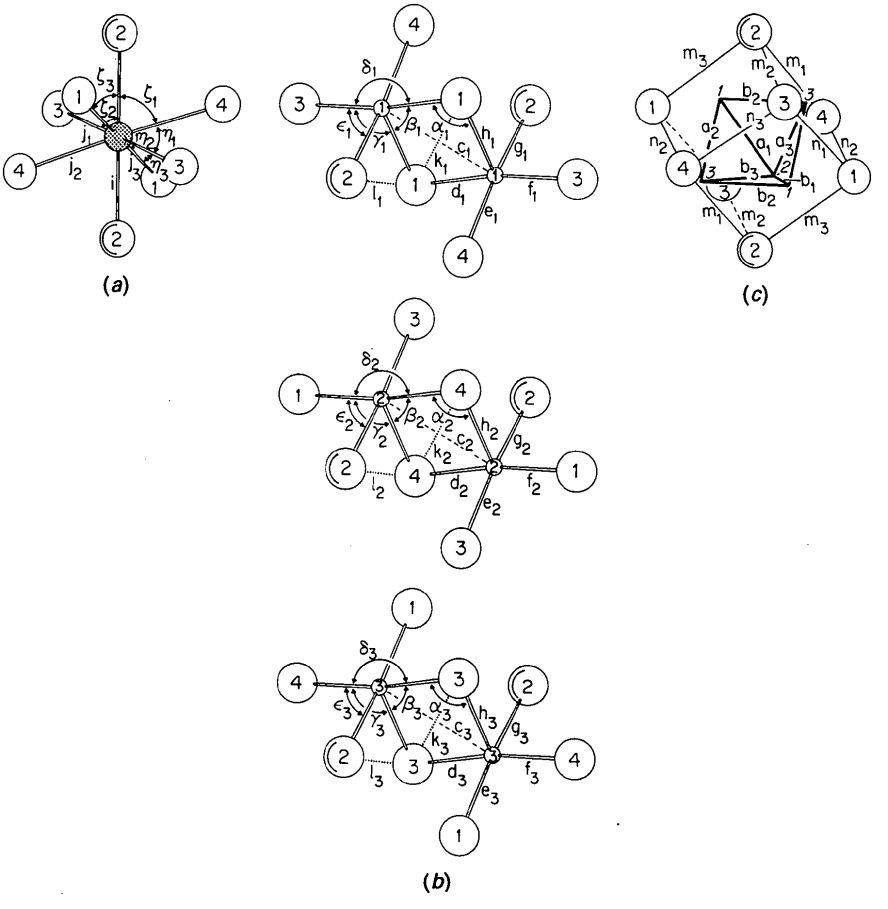

Fig. 2. Partial structure of triclinic $EuMo_6S_8$ and $BaMo_6S_8$ as viewed approximately parallel to the pseudoternary axis (numbers near atom sites indicate atom labels of Table 2): (*a*) environment of Eu(Ba), (*b*) chalcogen atom environment of Mo, (*c*) Mo_6 cluster. Mo: small circles, S: large open circles, Eu(Ba): shaded circles; Mo—Mo bonds: thick lines, Mo—S and Eu(Ba)—S bonds: double lines, S—S contact distances: single lines (*c*), dotted lines (*b*). For bond distances see Table 3.

than $\Delta V \sim 0{\cdot}2$ Å^3, in agreement with high-resolution neutron diffraction data on that compound (Jorgensen & Hinks, 1986)

The structural changes on the atomic level in both compounds are characterized by a rearrangement of the octahedral Mo_6 clusters which undergo a triclinic deformation due to an electronic instability (Nohl, Klose & Anderson, 1982; Baillif, Dunand *et al.*, 1981). This deformation is transferred to the chalcogen network by short Mo—S bonds (Fig. 2*b*), and is possibly enhanced by matrix effects (Corbett, 1981; Kubel & Yvon, 1988). As can be seen from the bond labels in Fig. 2 and the interatomic distances listed in Table 3 the largest differences of the Mo—Mo, Mo—S and Eu(Ba)—S bond lengths and S—S contact distances between the rhombohedral high-temperature modification at 112 K (177 K) and the triclinic low-temperature modification at 40 K (173 K) of $EuMo_6S_8$ ($BaMo_6S_8$) are 0·041 (0·033) Å (Mo—Mo, label b_3), 0·032 (0·021) Å (Mo—S, label g_1), 0·033 (0·028) Å [Eu(Ba)—S, label j_3] and 0·084 (0·066) Å [S—S, label m_1 (see part I)]. The largest differences between the bond lengths (contact distances) of the triclinic modification which are symmetry-equivalent in the rhombohedral modification, are for $EuMo_6S_8$ ($BaMo_6S_8$): 0·060 (0·044) Å [$(Mo—Mo)_{inter}$, label *c*], 0·068 (0·053) Å [$(Mo—Mo)_{intra}$, label *b*], 0·051 (0·040) Å (Mo—S, label *g*, *i.e.* the shortest Mo—S bond), 0·055 (0·048) Å [Eu(Ba)—S, label *j*], 0·131 (0·096) Å (S—S, label *m*). The shortest S—S contact distance in both compounds (label *l*) remains approximately constant during the phase transition, as expected from the role of the repulsive S—S interactions for the matrix effect (Corbett, 1981). The largest differences between the bond angles of the high- and low-temperature modification are for $EuMo_6S_8$ ($BaMo_6S_8$): 2·24 (1·69)° (S—Mo—S, bond label ε_3). The largest differences between the bond angles in the triclinic modification which are equivalent in the rhombohedral modification are for $EuMo_6S_8$ ($BaMo_6S_8$) 4·48 (3·27)° (S—Mo—S, label ε).

In conclusion, the structural changes during the rhombohedral-to-triclinic phase transition in $EuMo_6S_8$ and $BaMo_6S_8$ are relatively small, those in $EuMo_6S_8$ being slightly larger than those in $BaMo_6S_8$. In particular, the Mo—Mo bond distances which are of importance for the electronic properties presumably change only by as little as 0·03 Å at the phase transition. Theoretical band structure calculations (Nohl *et al.*, 1982) on preliminary structure data of triclinic $EuMo_6S_8$ have shown that such small differences are sufficient to explain the observed transition from metallic behavioiur at high temperatures to non-metallic behaviour at low temperatures. In view of these results it is likely that the appearance of superconductivity in that compound under pressure (Chu, Huang, Lin, Meng, Wu & Schmidt, 1981; Harrison, Lim, Thompson, Huang, Hambourger & Luo, 1981) is due to the suppression of the structural phase transition.

Table 3. *Interatomic distances and angles in* $EuMo_6S_8$ *and* $BaMo_6S_8$

		$EuMo_6S_8$				$BaMo_6S_8$			
Temperature (K)		112		40		177		173	
Space group		$R\bar{3}$		$P\bar{1}$		$R\bar{3}$		$P\bar{1}$	
Distances (Å)									
Mo—Mo	a*	2·7108 (8)	a_1†	2·6871 (13)	a*	2·6981 (15)	a_1†	2·6855 (16)	
			a_2	2·6836 (10)			a_2	2·6932 (14)	
			a_3	2·7342 (15)			a_3	2·7249 (16)	
	b	2·6593 (8)	b_1	2·6328 (14)	b	2·6649 (15)	b_1	2·6450 (16)	
			b_2	2·6342 (12)			b_2	2·6512 (15)	
			b_3	2·7003 (12)			b_3	2·6982 (14)	
	c	3·2652 (8)	c_1	3·2998 (13)	c	3·4091 (15)	c_1	3·4209 (15)	
			c_2	3·2398 (15)			c_2	3·3765 (17)	
			c_3	3·2852 (11)			c_3	3·4036 (14)	
Mo—S	d	2·5041 (17)	d_1	2·5306 (24)	d	2·498 (3)	d_1	2·504 (3)	
			d_2	2·5022 (23)			d_2	2·495 (3)	
			d_3	2·482 (3)			d_3	2·482 (4)	
	e	2·4596 (18)	e_1	2·480 (3)	e	2·468 (4)	e_1	2·487 (4)	
			e_2	2·4544 (22)			e_2	2·464 (3)	
			e_3	2·447 (3)			e_3	2·451 (4)	
	f	2·4461 (17)	f_1	2·4637 (25)	f	2·454 (3)	f_1	2·471 (3)	
			f_2	2·4404 (25)			f_2	2·451 (3)	
			f_3	2·436 (3)			f_3	2·446 (4)	
	g	2·3899 (25)	g_1	2·422 (3)	g	2·3874 (23)	g_1	2·408 (4)	
			g_2	2·3712 (21)			g_2	2·368 (3)	
			g_3	2·375 (3)			g_3	2·374 (4)	
	h	2·5768 (17)	h_1	2·5943 (23)	h	2·620 (3)	h_1	2·625 (3)	
			h_2	2·589 (3)			h_2	2·617 (4)	
			h_3	2·5837 (23)			h_3	2·623 (3)	
Eu(Ba)—S	i	2·830 (3)	i	2·842 (3)	i	2·9629 (14)	i	2·969 (3)	
	j	3·0877 (17)	j_1	3·0663 (25)	j	3·206 (3)	j_1	3·186 (3)	
			j_2	3·0729 (22)			j_2	3·193 (3)	
			j_3	3·121 (3)			j_3	3·234 (3)	
S—S	k	3·8933 (23)	k_1	3·922 (3)	k	3·819 (5)	k_1	3·824 (4)	
			k_2	3·928 (4)			k_2	3·841 (5)	
			k_3	3·857 (4)			k_3	3·808 (5)	
	l	3·399 (4)	l_1	3·414 (4)	l	3·400 (4)	l_1	3·407 (5)	
			l_2	3·414 (4)			l_2	3·400 (5)	
			l_3	3·395 (3)			l_3	3·398 (4)	
	m	3·4738 (21)	m_1	3·390 (3)	m	3·457 (3)	m_1	3·391 (5)	
			m_2	3·501 (4)			m_2	3·485 (5)	
			m_3	3·521 (3)			m_3	3·487 (4)	
	n	3·4379 (23)	n_1	3·381 (3)	n	3·462 (5)	n_1	3·418 (4)	
			n_2	3·467 (5)			n_2	3·463 (5)	
			n_3	3·481 (3)			n_3	3·495 (4)	
Angles (°)									
Mo—S—Mo	α	79·97 (5)	α_1	80·15 (7)	α	83·51 (10)	α_1	83·63 (10)	
			α_2	79·02 (8)			α_2	82·63 (9)	
			α_3	80·83 (9)			α_3	83·57 (11)	
S—Mo—S	β	100·03 (6)	β_1	99·85 (8)	β	96·49 (11)	β_1	96·37 (10)	
			β_2	100·98 (10)			β_2	97·37 (11)	
			β_3	99·17 (8)			β_3	96·43 (10)	
S—Mo—S	γ	88·64 (6)	γ_1	87·28 (8)	γ	91·36 (11)	γ_1	90·70 (10)	
			γ_2	88·10 (9)			γ_2	91·21 (11)	
			γ_3	89·52 (9)			γ_3	91·89 (11)	
S—Mo—S	δ	171·17 (7)	δ_1	172·69 (8)	δ	172·13 (12)	δ_1	172·86 (11)	
			δ_2	170·78 (11)			δ_2	171·41 (13)	
			δ_3	171·22 (8)			δ_3	171·66 (11)	
S—Mo—S	ε	91·82 (6)	ε_1	91·54 (9)	ε	91·11 (9)	ε_1	91·16 (11)	
			ε_2	94·05 (8)			ε_2	92·69 (11)	
			ε_3	89·58 (10)			ε_3	89·42 (12)	
S—Eu(Ba)—S	ξ	71·80 (7)	ξ_1	71·98 (6)	ξ	72·12 (6)	ξ_1	72·13 (8)	
			ξ_2	71·42 (8)			ξ_2	71·53 (9)	
			ξ_3	72·03 (8)			ξ_3	72·51 (8)	
S—Eu(Ba)—S	η	69·29 (4)	η_1	70·34 (6)	η	68·99 (8)	η_1	69·70 (7)	
			η_2	68·78 (8)			η_2	68·64 (8)	
			η_3	68·72 (6)			η_3	68·80 (8)	

* Bond labels *a*, *b*, *c etc.* of the rhombohedral modification refer to Fig. 2 of part I.

† Bond labels a_1, a_2, a_3 *etc.* of the triclinic modification are shown in Fig. 2.

We thank Dr R. Bailliff for supplying samples, Dr A. Dunand for single-crystal diffraction measurements and Dr J. Ihringer for powder diffraction measurements on $BaMo_6S_8$ at low temperature. The help of Mrs B. Künzler with the drawings is gratefully acknowledged. This work was supported by the Swiss National Science Research Foundation under contract No. 2.035–0.86.

References

BAILLIF, R., DUNAND, A., MULLER, J. & YVON, K. (1981). *Phys. Rev. Lett.* **47**, 672–675.
BAILLIF, R., JUNOD, A., LACHAL, B., MULLER, J. & YVON, K. (1981). *Solid State Commun.* **40**, 603–606.
CHU, C. W., HUANG, S. Z., LIN, C. H., MENG, R. L., WU, M. K. & SCHMIDT, P. H. (1981). *Phys. Rev. Lett.* **46**, 276–279.
CORBETT, J. D. (1981). *J. Solid State Chem.* **39**, 56–74.
DECROUX, M., TORIKACHVILI, M. S., MAPLE, M. B., BAILLIF, R., FISCHER, Ø. & MULLER, J. (1983). *Phys. Rev. B*, **28**, 6270–6276.
FRENZ, B. A. (1983). *Enraf–Nonius Structure Determination Package*. Enraf–Nonius, Delft, The Netherlands.
GELATO, L. M. & PARTHÉ, E. (1987). *J. Appl. Cryst.* **20**, 139–143.
HARRISON, D. W., LIM, K. C., THOMPSON, J. D., HUANG, C. Y., HAMBOURGER, P. D. & LUO, H. L. (1981). *Phys. Rev. Lett.* **46**, 280–283.
HOR, P. H., WU, M. K., LIN, T. H., SHAO, X. Y., JIN, X. C. & CHU, C. W. (1982). *Solid State Commun.* **44**, 1605–1607.
IHRINGER, J. (1982). *J. Appl. Cryst.* **15**, 1–4.
International Tables for X-ray Crystallography (1974). Vol. IV. Birmingham: Kynoch Press. (Present distributor Kluwer Academic Publishers, Dordrecht.)
JORGENSEN, J. D. & HINKS, D. G. (1986). *Physica*, **136B**, 485–488.
KUBEL, F. & YVON, K. (1987). *Acta Cryst.* C**43**, 1655–1659.
KUBEL, F. & YVON, K. (1988). *J. Solid State Chem.* **73**, 188–191.
KUBEL, F., YVON, K., IHRINGER, J. & WERNER, P.-E. (1988). *Phys. Rev. B*, **37**, 5814–5816.
LACHAL, B., BAILLIF, R., JUNOD, A. & MULLER, J. (1983). *Solid State Commun.* **45**, 849–851.
NOHL, H., KLOSE, W. & ANDERSON, O. K. (1982). *Superconductivity in Ternary Compounds* I, edited by Ø. FISCHER & M. B. MAPLE. Berlin: Springer Verlag.
PEÑA, O., HORYN, R., GEANTET, C., GOUGEON, P., PADIOU, J. & SERGENT, M. (1986). *J. Solid. State Chem.* **63**, 62–69.
STEWART, J. M., MACHIN, P. A., DICKINSON, C. W., AMMON, H. L., HECK, H. & FLACK, H. (1976). The *XRAY76* system. Tech. Rep. TR-446. Computer Science Center, Univ. of Maryland, College Park, Maryland, USA.

Acta Cryst. (1990). C**46**, 186–189

Structure Investigation by Neutron Diffraction of Deuterated Cobalt Fluosilicate Hexahydrate

BY G. CHEVRIER

Laboratoire Léon Brillouin, CEN-Saclay*, 91191 *Gif-sur-Yvette CEDEX, France*

AND R. SAINT-JAMES

Laboratoire de Physique du Solide et de Résonance Magnétique, CEN-Saclay, 91191 *Gif-sur-Yvette CEDEX, France*

(*Received* 25 *July* 1988; *accepted* 18 *May* 1989)

Abstract. Cobalt hexafluorosilicate–deuterium oxide (1/6), $CoSiF_6.6D_2O$, $M_r = 321$, trigonal, $R\bar{3}$, $a = 9{\cdot}369$ (10), $c = 9{\cdot}731$ (10) Å, $V = 740$ (2) Å^3, $Z = 3$, $D_x = 2{\cdot}16$ g cm^{-3}, $\lambda = 0{\cdot}8307$ (5) Å, $\mu = 0{\cdot}430$ cm^{-1} (evaluated), $F(000) = 46{\cdot}6$, room temperature, final R factor 0·070 for 506 observed reflections, $wR = 0{\cdot}034$. The structure determined by X-ray diffraction on a hydrogenated crystal is almost confirmed. The F atoms of the disordered SiF_6 octahedra have the same occupation probability (0·5/0·5). The configuration of the water molecule is perfectly determined: the distances D—O are 0·943 (2) and 0·947 (2) Å and the angle D—O—D is 109·1 (3)°. The lengths of the hydrogen bonds are 1·789 (3) and 1·968 (3), and 1·786 (4) and 1·835 (4) Å for D(1)···F and D(2)···F, respectively. When the temperature is lowered $CoSiF_6.6D_2O$ undergoes a structural phase transition with a large hysteresis between 268·1 (2) and 254·1 (2) K.

Introduction. The fluosilicates $MSiF_6.6H_2O$ (M = divalent metal) are now well known to present structural disorder. The two complex ions $M(H_2O)_6^{2+}$ and SiF_6^{2-} have an octahedral structure and can be distributed between two orientations around the three-fold axis. In the case of $MgSiF_6.6H_2O$ ($T \geq 300$ K) and $FeSiF_6.6H_2O$ (at room temperature), a structural model involving two types, with equal probability, of ordered domains (space group $P\bar{3}$) (Jehanno & Varret, 1975; Chevrier & Jehanno, 1979; Chevrier, Hardy & Jehanno, 1981) can explain the superstructure peaks which were inconsistent with the structure

* Laboratoire commun CEA-CNRS.

0108-2701/90/020186-04$03.00